

Understanding the structure of transparent zirconia glasses

Neutron Physics Laboratory - Neutron diffraction

Gennady Kopitsa

Proposal ID

23

Title. Understanding the structure of transparent zirconia glasses

Objectives. Transparent amorphous oxide glasses are considered to be very promising materials for photochromic devices, catalytic systems, chemical sensors, etc. These materials are also proposed as matrices for thermally stable luminescent nanocomposites (containing either II-VI semiconductor nanoparticles of rare-earth compounds) and non-linear optics devices, especially lasers. Up to now, amorphous glasses were mostly made from silica and due to this reason the range of their possible applications was considerably limited. Recently we've succeeded in development of sol-gel technique of transparent zirconia glasses possessing very high surface area (up to 400 m²/g). The method proposed doesn't include supercritical drying stage, so it's truly low cost and efficient.

Thus, the aim of the present study was to investigate for the first time the mesostructure of transparent porous zirconia glasses formed by sol-gel technique and to elucidate reliably the possibility of fine tuning of their characteristics. This task is supposed to be solved by using both USANS, SANS and complementary methods (TEM, XRD, TGA/DTA/DSC, etc.).

Experiment

1. Samples. Six series of the samples of zirconia glasses prepared by slow hydrolysis of zirconium propoxide in the presence of water, nitric and hydrochloric acids, isopropanol, dimethylformamide, acetylacetone etc. were studied.

2. USANS. The HR-SANS experiment was performed at the double-crystal diffractometer MAUD of LVR-15 research reactor in Prague (Czech Republic), which using neutrons with the wavelengths $\lambda = 2.09 \text{ \AA}$ ($\Delta\lambda/\lambda = 0.18$). The range of momentum transfer $2.5 \cdot 10^{-4} < q < 4 \cdot 10^{-3} \text{ \AA}^{-1}$. All measurements were made at room temperature.

Achievements and Main Results. Figure 1 shows the experimental $d\Sigma(q)/d\Omega$ vs. q curves for zirconia glasses prepared by slow hydrolysis of zirconium propoxide in isopropanol-based media with various water content at room temperature (Fig. 1a) and $T = 0^\circ\text{C}$ (Fig. 1b). These data clearly demonstrate that small-angle scattering for $\text{ZrO}_2 \times x\text{H}_2\text{O}$ glasses depends upon both water content and the temperature of synthesis.

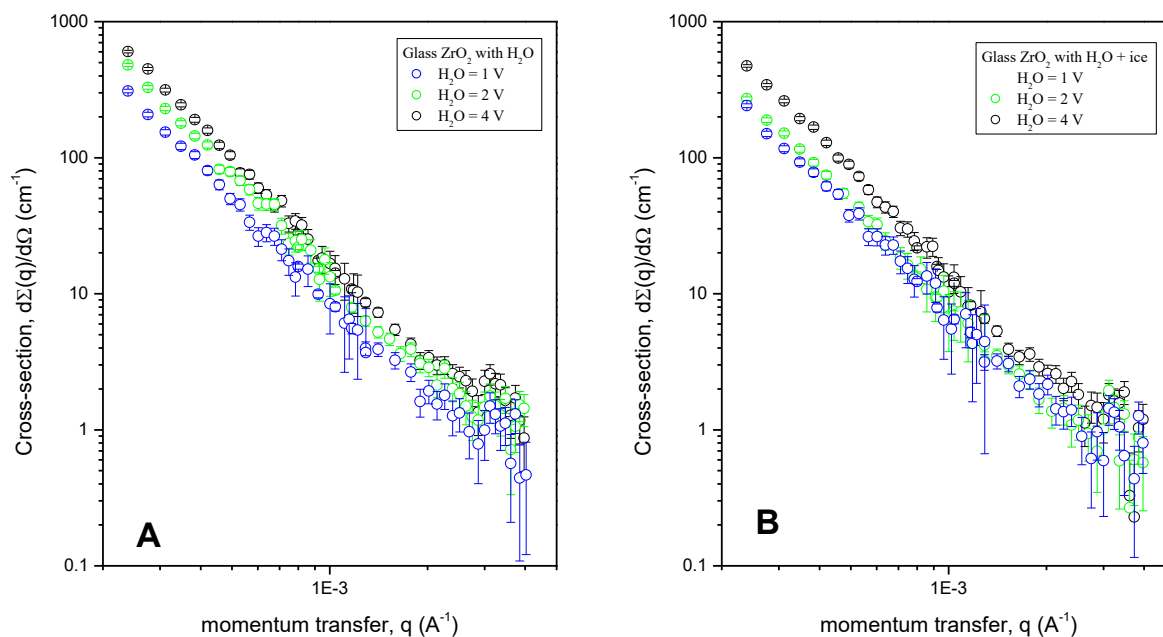


Figure 1. Experimental $d\Sigma(q)/d\Omega$ vs. q curves for zirconia glasses

The treatment of USANS data for samples of zirconia glasses prepared by slow hydrolysis of zirconium propoxide in the presence of water, nitric and hydrochloric acids, isopropanol, dimethylformamide, acetylacetone etc. and interpretation of all the data obtained is still in progress.

Inner structure of the basic element of large sintered artificial opals

Neutron Physics Laboratory - Neutron diffraction

Gennady Kopitsa

Proposal ID

25

EXPERIMENTAL REPORT

Title. Inner structure of large sintered artificial opals

Objectives. The experiment aims the structural characterization of new material made on the base of silicon dioxide spheres synthesized by modified Stober method. The diameter spheres is varied from 320 nm to 2200 nm in different samples with monodispersity better than 5%. In previous SAS experiments we determined that this spheres have initial particles with size 7-10 nm. It is obtained from SEM at higher contrast and magnification demonstrates the edge of the cross-section of the particle having the several undeformed secondary particles of size of order 60 nm of quasi-sphere, or oval shapes[1]. The experiment goal was to uniquely determine by non-destructive method (HR-SANS) if there are secondary particles.

Experiment

1. Samples. Silica particles were prepared using the modified Stöber method by the tetraethylorthosilicate (TEOS) hydrolysis reaction in aqueous-alcoholic solution in the presence of ammonium hydroxide (50% vol. ethanol, 1.0 M ammonium).

2. Ultra small-angle neutron scattering. The HR-SANS experiment was performed at the double-crystal diffractometer MAUD of LVR-15 research reactor in Prague (Czech Republic), which using neutrons with the wavelengths $\lambda = 2.09$ nm ($\Delta\lambda/\lambda = 0.18$). The range of momentum transfer $2 \times 10^{-4} < Q < 2 \times 10^{-2}$ \AA^{-1} .

All measurements were made at room temperature.

Achievements and Main Results. The inner structure was studied by USANS method. There are scattering curves in double logarithmic scale on the figure 1. These data clearly demonstrate that small-angle scattering depends on sphere diameters.

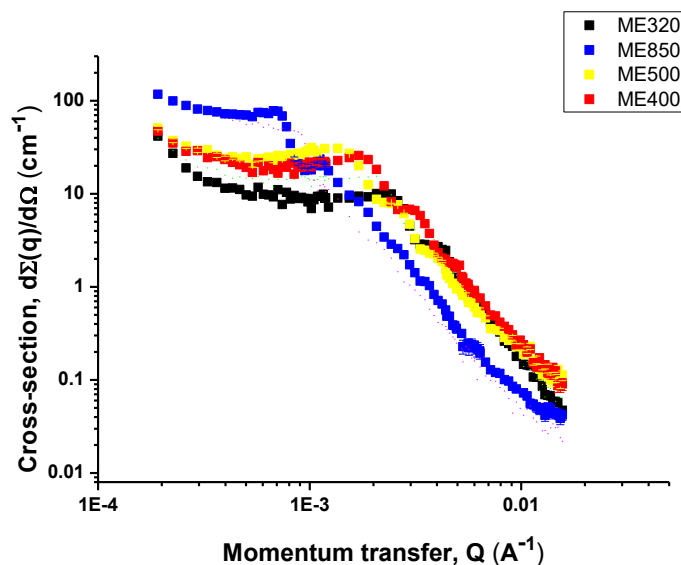


Fig. 1 The HR-SANS cross section $d\Sigma(q)/d\Omega$ for the samples of silica particles with different diameters (■ - 320, ■ - 400, ■ - 500, ■ - 850 nm)

The treatment of SANS data for samples of artificial opal and interpretation of all the obtained data is still in progress.

References

[1] V.M. Masalov et. al. Direct observation of the shell-like structure of SiO₂ particles synthesized by the multistage Stöber method. NANO: Brief Reports and Reviews Vol. 8, No. 4 (2013)

Neutron based analytical methods for investigation of carbon based materials

Neutron Physics Laboratory - Nuclear analytical methods with neutrons

Zdenek Sofer

Proposal ID

19

Project Title: Neutron based analytical methods for investigation of carbon based materials

Proposer: Zdenek Sofer (zdenek.sofer@vscht.cz)

Lab: Neutron Physics Laboratory - Nuclear analytical methods with neutrons

NAA method was used for the evaluation of impurities concentration in graphene and graphene oxide which were prepared by various methods. Metallic impurities have significant effect on electrochemical properties and subsequent applications of carbon nanomaterials. Such as in case of carbon nanotubes (CNT) the electrochemical properties are dominated by electrochemical properties of metallic impurities. High purity graphite was used in order to avoid introduction of impurities to the starting material. Starting graphite oxides were prepared by Brodie, Staudenmaier, Hofmann and Hummers methods. Various methods led to the introduction of impurities related to the chemicals used for oxidation. High concentration of manganese was observed in graphene oxide and also graphite prepared by Hummers method. In all graphite oxides and graphenes high concentrations of alkali metals (sodium and potassium) were measured. The increase of impurities concentration was observed during the whole process (oxidation of graphite and subsequent reduction). In this case graphene oxides acted as a sorption material and they concentrated various metals. Their concentration was further increased during the reduction of graphene oxide (chemical and thermal reduction). During the reduction process oxygen functional groups are removed and impurities are concentrated within graphene. Other methods like PIXE and ICP-OES were used for the comparison of results obtained by NAA. NAA method is the most suitable for elements with high cross section of thermal neutrons. PIXE has a very low sensitivity for light elements. For ICP-OES analysis the sample must be dissolved and these procedures often introduce significant deviations in the analysis results.

The obtained concentrations of metallic impurities were correlated with the results of ICP-OES (which gave lower results) and PIXE. Based on the analytical results the electrochemical measurement (cyclic voltammetry) with various redox probes was performed. The redox probes with high sensitivity towards metallic impurities were tested (like hydrogensulphide ions and cumene hydroperoxide) and also standard redox probe ($[\text{Fe}(\text{CN})_6]^{3-/4-}$) was used for calculation of heterogeneous electron transfer (HET) rate.

Obtained results are evaluated and they will be published in impacted journal within six months.

Structure of new silica, alumina, and zirconia aerogels with unusual properties

Neutron Physics Laboratory - Neutron diffraction

Gennady Kopitsa

Proposal ID

22

Title. Structure of new silica, alumina and zirconia aerogels with unusual properties

Objectives. Aerogels are unique mesoporous materials having more than 90% porosity. The structure of aerogels corresponds to ramified network of nanoparticles clusters with 10–100 nm pores. Extremely high porosity and low density of aerogels results in their low thermal conductivity and high thermal stability – up to 1200°C. These materials are excellent heat and sound insulators and have proved to be effective heterogeneous catalysts. Nanomaterials based on noble metal or intermetallic nanoparticles introduced in aerogel matrices are considered also as hydrogen storage materials.

The aim of the present study is to investigate the mesostructure of SiO₂, Al₂O₃, ZrO₂ aerogels formed by the novel supercritical drying technique and to gain information on their fractal characteristic, aggregate structure, porosity, etc. This task is supposed to be solved by using complementary methods (TEM, XRD, TGA/DTA/DSC, etc.).

Experiment

1. Samples. Series of the samples of SiO₂, Al₂O₃, ZrO₂ aerogels prepared by the novel technique of supercritical drying gel using different solvents like ethanol, hexafluoroisopropanol, diethyl ether and methyl tert-butyl ether.

2. USANS. The HR-SANS experiment was performed at the double-crystal diffractometer MAUD of LVR-15 research reactor in Prague (Czech Republic), which using neutrons with the wavelengths $\lambda = 2.09 \text{ \AA}$ ($\Delta\lambda/\lambda = 0.18$). The range of momentum transfer $2.5 \cdot 10^{-4} < q < 1.2 \cdot 10^{-2} \text{ \AA}^{-1}$. All measurements were made at room temperature.

Achievements and Main Results. Mesostructure of aerogels was studied by USANS and SANS methods. Figure 1 shows the experimental $d\Sigma(q)/d\Omega$ vs. q curves for aerogels based on zirconia prepared by using different solvents (ethanol(EtOH), hexafluoroisopropanol(HFIP) and diethyl ether(Et₂O)). These data clearly demonstrate that small-angle scattering depends on using solvents.

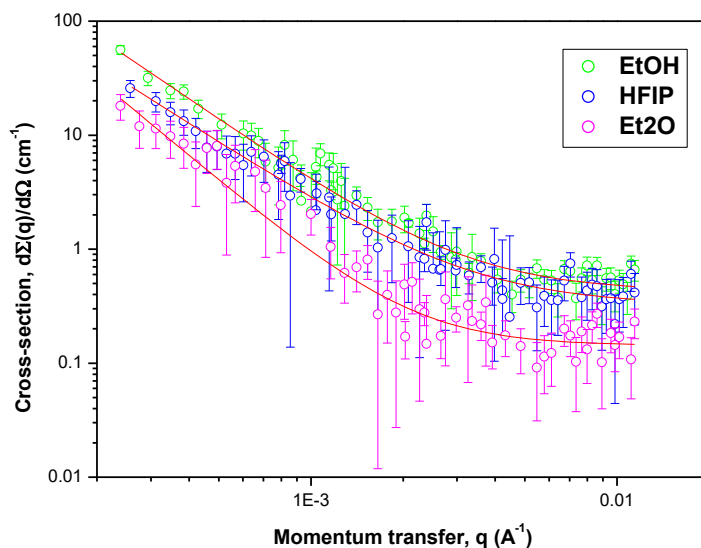


Figure 1. Experimental $d\Sigma(q)/d\Omega$ vs. q curves for aerogels based on zirconia with using different solvents (ethanol(EtOH), hexafluoroisopropanol(HFIP) and diethyl ether(Et₂O)).

It is clearly seen that $d\Sigma(q)/d\Omega$ for all samples satisfies the power law q^{-n} . For aerogels prepared with using ethanol(EtOH) and hexafluoroisopropanol (HFIP) solvents the exponent n values are equal 1.7 and 1.85. It means that the scattering from these aerogels occurs on the volume fractals with the dimensions $D_V = n + 1 \approx 2.7$ and 2.85, respectively. In the case of the aerogel prepared with using diethyl ether (Et₂O) solvent the exponent $n \approx 2.3$. This corresponds to the scattering from the fractal surface with the dimension $D_s = 6 - (n+1) = 2.7$.

The treatment of SANS data for samples of SiO₂, Al₂O₃, ZrO₂ aerogels and interpretation of all the obtained data is still in progress.

Effect of high LET radiation on specific interaction of proteins with DNA.

Laboratory of Cyclotron and Fast Neutron Generators

Marie Davidkova

Proposal ID

21

Průběžná zpráva o realizaci projektu za rok 2012

Projekt je řešen jako příspěvek řešitelského týmu k mezinárodnímu projektu COST MP1002 "Nano-scale insights in ion beam cancer therapy (Nano-IBCT, Nano-aspekty iontové terapie nádorů)". Řešitelská laboratoř je součástí pracovní skupiny WG5 Radiobiologické efekty (detekce dvojných zlomů DNA, predikce a buněčné projevy poškození). Cílem projektu je určit jakým způsobem ovlivňuje radiační poškození reparačních proteinů rychlost a správnost reparačních mechanismů v buňkách.

Ozařování biologických vzorků na urychlovačích v ÚJF v Řeži, cyklotron U120M a tandetron, je specifické díky energiím dostupných nabitých částic. Maximální energie protonů na cyklotronu U120M je přibližně 34 MeV, na tandetronu 6 MeV. Dosah těchto iontů ve vodě je pouze několik desítek μm až mm (protony 6 MeV mají ve vodě dosah přibližně 0,5 mm, 34 MeV 11 mm), proto je třeba pracovat s tenkými vrstvičkami vzorků.

Bylo navrženo a testováno několik možných řešení:

- a) Prototypové plastové nebo kovové kroužky držící velmi tenkou Mylar folii vyrobené v ODZ ÚJF
- b) Sterilní Petriho misky s kruhovým otvorem ve dně, na které je nalepeno krycí mikroskopické sklíčko
- c) Komerčně dostupné plastové misky, u kterých je dno a případně i víčko nahrazeno Mylar folií (firma Chemplex, USA).

Navržená řešení byly testovány během ozařování na cyklotronu U120M. Pro další experimenty s neonatálními dermálními fibroblasty se jeví jako nejvhodnější řešení varianta c. Pro experimenty realizované ve spolupráci s kolegy z Biofyzikálního ústavu AV ČR v Brně, kdy byly buňky analyzovány metodou FISH (fluorescenční in situ hybridizace) se jeví výhodnější uspořádání v Petriho miskách (varianta b). Buňky rostou přímo na mikroskopickém sklíčku, po ozáření jsou dále zpracovány a analyzovány fluorescenčním mikroskopem. DNA ve vodných roztocích jsou ozařovány v úzkých plastových mikrozkuřkách.

Podíl přímého a nepřímého účinku ve stopách protonů byl studován s použitím DNA plasmidů pBR322 ve vodných roztocích. Vzorky obsahovaly různé koncentrace sloučenin vychytávající hydroxylové radikály (kumarin-3-karboxylová kyselina, dimethylsulfoxid nebo glycyglycin). Metodou agaróзовé elektroforézy byly stanoveny výtěžky jednoduchých a dvojných zlomů DNA. V závislosti na koncentraci vychytávače lze odhadnout podíl přímého poškození DNA a příspěvek nepřímého poškození prostřednictvím OH radikálů. Tyto informace budou velmi zajímavým výstupem projektu, zvláště pokud získáme větší rozsah různých iontů a energií.

Radiační poškození proteinů bylo studováno u restričních enzymů HindIII a PvuII. Enzymy ozářené rostoucími dávkami záření byly inkubovány s pCDNA3 plasmidy a vzorky byly poté analyzovány metodou agaróзовé elektroforézy. Funkční enzymy rozpoznávají specifickou sekvenci bází a v tomto místě DNA štěpí. Proteiny poškozené zářením postupně ztrácejí schopnost rozpoznat a štěpit DNA. Bylo sledováno snižování aktivity enzymů s rostoucí dávkou záření.

V prvním roce řešení projektu nebylo plánováno získání výsledků pro buněčné kultury. V rámci přípravy byly nicméně připraveny metodiky pro realizaci experimentů, potřebné laboratorní uspořádání a byly realizovány první pilotní experimenty. Křivky přežití byly měřeny pro konfluentní neonatální fibroblasty pěstované na 2,5 μm Mylar foliích a ozářených rostoucími dávkami gama záření a 15 a 30 MeV protonů. V ozářených vzorcích bylo stanoveno přežití buněk a četnost výskytu mikrojader. Experimenty budou zopakovány, doplněny a analyzovány. Ve spolupráci s Biofyzikálním ústavem AV ČR, v.v.i. proběhly i první experimenty zaměřené na reparaci DSB v neonatálních fibroblastech v závislosti na struktuře chromatinu v buněčném jádru.

Characterization of impurities in carbon nanomaterials

Laboratory of Tandetron

Zdenek Sofer

Proposal ID

16

Project Title: Characterization of impurities in carbon nanomaterials

Proposer: Zdenek Sofer (zdenek.sofer@vscht.cz)

Lab: Laboratory of Tandetron

Measurements in Tandetron laboratory were used for RBS/ERDA and also PIXE analysis. The RBS method was used for the characterization of carbon nanomaterials (measurement of C/O/H ratio) and also semiconductor thin films implanted with rare earths and transition metals (GaN and ZnO).

The deep concentration profiles and total amount of Gd ions with ZnO substrates were measured. The RBS measurement was also used to evaluate the damage induced by ion implantation and further recovery of layered structure by annealing in various atmospheres. The ZnO layers were also characterized by Raman spectroscopy, SQUID magnetometry and AFM measurements. Obtained results were correlated with data from RBS. The ferromagnetism was observed only for as gadolinium implanted ZnO substrates and subsequent annealing led to paramagnetic behavior. From this results we can conclude that in the case of ZnO the exotic ferromagnetism is correlated to the presence of ion implantation induced defects and possible presence of gadolinium nanoclusters. RBS measurements were used also for the characterization of GaN thin films implanted with various rare earths elements (Ho, Tb and Tm). The RBS method was used to measure concentration profiles and for the estimation of total dose of implanted ions. The partial recovery of layered structure was observed after high temperature treatment of the layer. Formation of defects on the layer surface was observed for the doses over 1×10^{16} at.cm⁻² (at 200 keV energy).

The RBS/ERDA method was used for the measurement of C/H/O ratios in graphene based materials. Results were correlated to the data obtained by elemental combustion analysis. In the case of RBS higher C/O ratio was observed. This is related to the partial decomposition of graphene and further removed oxygen functionalities due to the interaction with ion beam used for measurements. The PIXE and PIGE methods were used to measure heavy and light elements concentration, respectively. The concentration of boron was correlated with results obtained by PG-NAA. The concentrations of metallic impurities obtained by PIXE were correlated to the concentrations obtained by ICP-OES and NAA. In comparison to ICP-OES method, PIXE had advantages related to easier sample preparation for analysis. For the ICP-OES the sample must be decomposed and transferred to the solution by combustion and acid digestion. This procedure is not sufficiently effective and lower concentrations of metallic impurities are often observed. Obtained results were compared to data obtained by ICP-OES and NAA and subsequently correlated to the electrochemical characterizations. The results of PIXE and RBS/ERDA measurement of graphene will be published within six months.

Published results:

A. Mackova, P. Malinský, Z. Sofer, P. Šimek, D. Sedmidubský, M. Mikulics: A Study of the Structural properties of GaN implanted by various rare-earth ions, Nuclear Instruments and Methods in Physics Research Section B: Beam Interactions with Materials and Atoms, 307 (2013) 446-451.

Mackova, P. Malinský, Z. Sofer, P. Šimek, D. Sedmidubský, M. Mikulics, R. A. Wilhelm: A Study of the Structural and Magnetic Properties of ZnO Implanted by Gd Ions, Nuclear Instruments and Methods in Physics Research Section B: Beam Interactions with Materials and Atoms, accepted.

RNAA for selenium determination in wheat samples

Neutron Physics Laboratory - Nuclear analytical methods with neutrons

Catarina Galinha

Proposal ID

15

Background

Cereals are an important component on human nutrition and are considered a good source of proteins and one of the major dietary sources of selenium (Se) when it is available at soil. Different methods of selenium supplementation were used. Foliar addition in two different growth stages (booting and grain filling), the addition of selenium to soil prior to sowing and selenium enriched seeds. Selenium in wheat samples were analysed by INAA (Instrumental Nuclear Activation Analysis), and CINAA (cyclic INAA) on the fast pneumatic system (SIPRA) available at the Portuguese Nuclear Reactor (RPI), using respectively ^{75}Se and $^{77\text{m}}\text{Se}$. The values of selenium were below the detection limit, and values could not be determined.

Experimental

Samples from soil supplementation, reference materials, blank ampoules and standards were irradiated in the LVR-15 light-water reactor for 20 h. The irradiated samples were allowed to cool for 1 month. After separation the samples were measured with a well-type HPGe detector for 2 h. The Se separation yield was determined through reactivation of a carrier by short-time irradiation (30 s) in a pneumatic facility, and counting of the $^{77\text{m}}\text{Se}$ radioisotope with a coaxial HPGe detector. For quantification of Se contents in the samples an irradiated liquid ^{75}Se standard was used.

Results and Discussion

The experiment was extremely well executed. Due to a very high yield and selectivity of the Se chemical separation RNAA is a very suitable method to achieve Se in samples where this element has very low concentrations. Table 1 resumes the values determined within this study.

Table 1. Selenium concentrations attained for the analyzed samples.

Type of Sample	Sample Code	[Se] (mg/kg)	Type of Sample	Sample Code	[Se] (mg/kg)
Bread Wheat	JBrancoFoliar	73	Soil	SoloGenerico	92
Bread Wheat	JBranco	43	Durum Wheat	MBrancoFoliar	167
Bread Wheat	RBranco	68	Durum Wheat	MBranco	44
Bread Wheat	SOJ4SA3	9	Durum Wheat	CBranco	34
Bread Wheat	SOJ4SAK12	10	Durum Wheat	SOM20SA3	26
Bread Wheat	SOJ4SIK12	12	Durum Wheat	SOM20SAK11	40
Bread Wheat	SOJ20SA1	23	Durum Wheat	SOM20SAK13	28
Bread Wheat	SOJ20SA2	57	Durum Wheat	SOM20SI4	12
Bread Wheat	SOJ20SI3	19	Durum Wheat	SOM20SI3	23
Bread Wheat	SOJ100SA1	126	Durum Wheat	SOM20SIK13	57
Bread Wheat	SOJ100SA2	28	Reference Material	RM 1515	51
Bread Wheat	SOJ100SA3	98	Reference Material	RM8433	42
Bread Wheat	SOJ100SAK11	791	Reference Material	RM 1515	40
Bread Wheat	SOJ100SAK12	530	Reference Material	RM 8433	40
Bread Wheat	SOJ100SAK13	280	Blank	BLANK	0

The results show that an increasing of the Se concentration used in the soil supplementation improves the Se content in the mature grains, and that this method of supplementation is not suitable using the rates of supplementation of 4 and 20gSe/ha, since there is no increase of Se in the grain.

The yield of chemical separation of Se in the RNAA procedure was very high (mean: 98%; standard deviation: 3.4%). However, a correction for the actual yield was employed. Accuracy of the procedure was done by analyzing the reference materials NIST-SRM 1515 and NIST-SRM 8433, showing an agreement between results of this work and NIST values.

Excitation functions of p-induced reactions on nat-Nd targets in the energy range 5-12MeV + 28-38MeV

Laboratory of Cyclotron and Fast Neutron Generators

Valentina Lozza

Proposal ID

13

Report on low energy and high energy proton activation of a natural Nd target.

Valentina Lozza, Johannes Petzoldt and Kai Zuber
Technical University of Dresden, 01069 Dresden, Germany

1 Introduction

^{150}Nd is one of the preferred candidate for neutrinoless double beta decay studies, with an isotopic abundance of 5.6% and a high Q-value, above most of the natural background. Nd can be activated, while it is on the surface, by cosmic neutrons and protons. The activation products, in some cases, are long living isotopes that can be a background for the $0\nu 2\beta$ -decay studies. In the case of p-induced reactions most of the production cross sections were not measured before and hence a verification of the theoretical data is necessary. In order to complete the investigation reported in [1], the 28-38 MeV range, and the 5-12 MeV range are explored. The measurement were performed at the LC of NPI-ASCR, in days from 12th to 13th of November 2012 and used as a target 4 natural Nd foils (99.9% purity, AlfaAesar) of $10 \times 10 \text{ mm}^2$ and 0.1 mm thickness for the high energy range, and 4 samples of the same area but smaller thickness (about 25 μm) for the low energy range. Since Nd oxidises very quickly in contact with air, the foils were covered by a thin layer of Parylene.

2 Thickness measurement

2.1 Thick natNd foils

The foil thickness was measured using low energy gamma ray (^{241}Am source) absorption at the Technical University of Dresden before the Parylene coating. To prevent oxidation the foil was measured in a mylar package under Argon atmosphere. The contribution of the mylar package was removed from the thickness measurement. Due to the large distance (more than 1 meter) between the sample and the detector (Ge-detector) the absorption coefficient with coherent scattering was used. The measurement was performed in different positions to test inhomogeneity in the foil itself. The average thickness is equal to $106 \pm 1 \text{ }\mu\text{m}$ (i.e. 74.31 mg/cm^2).

2.2 Thin natNd foils

The foil thickness was measured both at the TU Dresden and at the LC institute in Řež, due to the impossibility to measure the thickness before the irradiation without opening the protective package under nitrogen atmosphere. The measurement performed at Řež, used the same Ge-detector that will be used for the activated sample counting. A special holder in lead with a pinhole (nearly 1 mm diameter) was prepared for the measurement. The thickness measured is nearly constant for the 4 thin targets, and equal to 20 μm . 5 measurements of the foils and 2 measurement of a blank were performed. The presence of the parylene coating doesn't influence the measurement of the thickness, being the absorption in parylene negligible.

3 Irradiation

Both the thin and the thick foils were measured in a stack configuration. Typical stack arrangement is given below:

- Titanium (thickness 12.11 μm) acting as a beam monitor;
- Plastic-coated neodymium foil (thickness nearly 106 μm or 20 μm);
- Copper beam energy degrader (Cu thickness 10.6 μm);
- Titanium (thickness 12.11 μm) acting as a beam monitor;
- Plastic-coated neodymium foil (thickness nearly 106 μm or 20 μm);
- Copper beam energy degrader (Cu thickness 10.6 μm);
- Titanium (thickness 12.11 μm) acting as a beam monitor;
- Plastic-coated neodymium foil (thickness nearly 106 μm or 20 μm);
- Copper beam energy degrader (Cu thickness 10.6 μm);
- Titanium (thickness 12.11 μm) acting as a beam monitor;
- Plastic-coated neodymium foil (thickness nearly 106 μm or 20 μm);
- Thick silver foil acting as a beam stop, directly cooled by water.

The first stack arrangement had the following energy at the center of each Nd foil: 35.5 MeV, 33.39 MeV, 31.37 MeV, 29.84 MeV. The irradiation lasted for 1 hour at a beam current of 0.35 μA . The beam preparation required nearly 4 hours before the measurement took place. The foils were counted overnight after the measurement. The thin foils were irradiated on the forth day for about 2 hours at a beam current of 0.35 μA . The estimated currents at the center of each foil are: 9.23 MeV, 8.09 MeV, 6.81 MeV, 5.33 MeV. The samples were counted after the irradiation in order to catch also the short living isotopes.

References:

- [1] O. Lebeda et al., Phys. Rev. C 85 (2012) 014602

Assessment of the Impact of North Mara Gold Mine on River Mara Fish Contamination by Heavy Metals

Neutron Physics Laboratory - Nuclear analytical methods with neutrons

Najat Mohammed

Proposal ID

40

Samples of catfish (*Clarias mossambicus*) and lungfish (*Protopterus aethiopicus*) which are most consumed species of fish from River Mara in Tarime District of Mara Region were analyzed by INAA. Twenty samples of each fish species were collected from two sampling stations of Wegita (downstream) and Mrito (upstream) along River Mara at vicinity of North Mara Gold Mine (NMGM). The sampling stations were 70 km apart.

The samples were freeze dried, homogenized by cryogenic grinding and deep-frozen prior to analysis. Sample aliquots of approximately 100 mg and 200 mg for short-time and long-time irradiation, respectively, were sealed into acid-cleaned polyethylene disk-shaped capsules. Short- and long-time irradiations for 30 s and 3 h, respectively, were carried out in the LVR-15 reactor of the Research Centre Řež, Ltd. at neutron fluence rates of $3 \cdot 10^{13} \text{ cm}^2 \text{ s}^{-1}$, $1 \cdot 10^{13} \text{ cm}^2 \text{ s}^{-1}$, and $8 \cdot 10^{13} \text{ cm}^2 \text{ s}^{-1}$ for thermal, epithermal, and fast neutrons, respectively. Multielement standards containing known amounts of elements to be determined were simultaneously irradiated with the samples. For quality control purposes, NIST SRM 1577b Bovine Liver and NIST SRM 2711 Montana Soil were analyzed.

Counting of the irradiated samples and standards was performed in conditions given in Table 1, where t_i is irradiation time, t_d is decay time, t_c is counting time, and counting geometry is the distance of the sample from the cap of the detector. The samples and multielement standards were counted in the same geometry.

Table 1. Irradiation and counting conditions

t_i	t_d	t_c	Counting geometry	Detector ^a
30 s	10 min.	10 min.	15 cm	HPGe-1
3 h	4-5 days	1 h	20 cm	HPGe-2
	1 month	3 h	1 cm	HPGe-2

^a HPGe-1: coaxial HPGe detector with 23 % relative efficiency, resolution FWHM 1.80 keV for the 1332.5 keV photons of ⁶⁰Co

HPGe-2: coaxial HPGe detector with 53 % relative efficiency, resolution FWHM 1.80 keV for the 1332.5 keV photons of ⁶⁰Co

The detectors were coupled to Canberra Genie 2000 computer-controlled gamma spectrometer via the chain of linear electronics, which contained a loss-free counting module (LFC Canberra 599, dual mode) to correct for the pile-up effect and dynamic changes of dead time.

Fifteen elements which are Na, Cl, K, Ca, Sc, Cr, Mn, Fe, Co, Zn, Se, Br, Rb and Sr were detected in concentration above the Minimum Detection Limit (MDL) in samples of both fish species. The concentrations of toxic elements As, Cd, Th and U were found to be below MDL of the system used in this study. In this project Hg was not detected. Most of the elements were found to be in higher concentrations in samples from downstream than upstream which might indicate contamination from the nearby Gold mine.

Composition of the newly synthesized heavy-fermion compound Ce_2PtIn_8

Laboratory of Tandetron

Marie Kratochvílová

Proposal ID

42

Proposal Title: Composition of the newly synthesized heavy-fermion compound Ce_2PtIn_8

The aim of this proposal was to determine the stoichiometric composition of new single Ce-T-In crystals we have prepared. Characterization of samples using the energy dispersive *x*-ray analysis (EDX) in the mapping mode revealed the presence of two very similar, however clearly distinguishable phases with compositions close to 2:1:8 ratios. The stoichiometry of these phases could not be determined precisely using point EDX analysis. Neither the powder nor the single-crystal *x*-ray diffraction could resolve clearly the structure of both phases. To be able to determine the compositions of both phases precisely, we applied for experiment with accelerated ions provided by LT. The sensitivity of microprobe analysis was high enough to examine the surface morphology; unfortunately, it was not able to distinguish the presence of different phases. Later, we were able to prepare single crystalline samples of Ce_2PtIn_8 and $\text{Ce}_3\text{PtIn}_{11}$ with respect to new technological approach. The subsequent single-crystal *x*-ray diffraction and EDX analysis revealed homogeneous, single-phase composition of both tetragonal phases and thus, the issue with two phases of a very close composition within our samples (see Fig. 1) was resolved.

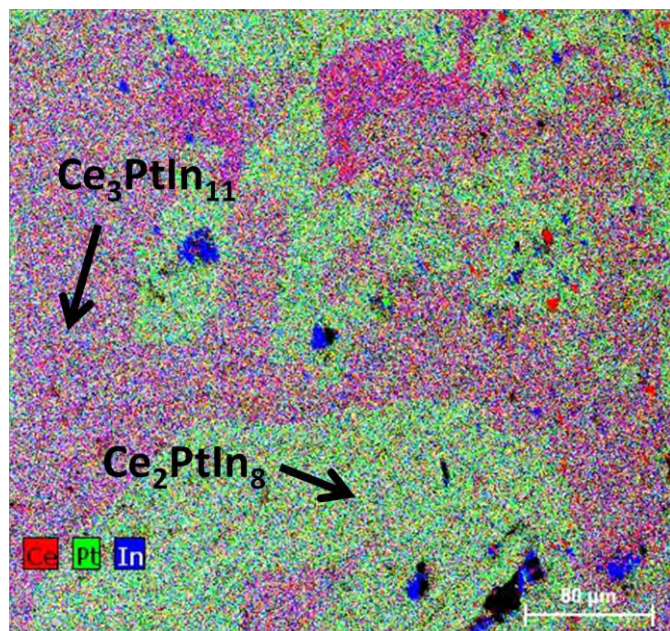


Fig. 1: EDX mapping pattern of multi-phase samples of both 2-1-8 and 3-1-11 composition. The green region represents the Ce_2PtIn_8 phase; the red region points to presence of the $\text{Ce}_3\text{PtIn}_{11}$ phase.

Surface analysis of plasma and laser modified substrates

Laboratory of Tandetron

Petr Slepika

Proposal ID

35

The following research topics have been studied:

a) Gold nanolayer and nanocluster coatings induced by heat treatment and evaporation technique

The preparation and surface characterization of gold coatings and nanostructures deposited on glass substrate was performed. Different approaches for the layer preparation were applied. The gold was deposited on the glass with (i) room temperature, (ii) glass heated to 300°C, and (iii) the room temperature-deposited glass which was consequently annealed to 300°C. The sheet resistance and concentration of free carriers were determined by the van der Pauw method. Surface morphology was characterized using an atomic force microscopy. The optical properties of gold nanostructures were measured by UV–vis spectroscopy. The evaporation technique combined with simultaneous heating of the glass leads to change of the sheet resistance, surface roughness, and optical properties of gold nanostructures. The electrically continuous layers are formed for significantly higher thickness (18 nm), if the substrate is heated during evaporation process. The annealing process influences both the structure and optical properties of gold nanostructures. The elevated temperature of glass during evaporation amplifies the peak of plasmon resonance in the structures, the surface morphology being significantly altered. The difference in surface metal distribution of evaporated structures under RT and evaporated onto substrate heated to 300°C is evaluated in Figure 1. The difference in the behavior of surface nanostructures in area on electrical discontinuity and continuity can be clearly seen. The electrically discontinuous layer exhibits significantly higher gold concentration when deposited on non-heated substrate. The heat treatment seems to be a positive promoter of surface diffusion (and nanocluster growth), mostly in the early stages of gold layer growth. This difference, thus, seems to affect the surface gold concentration; the higher the surface concentration, the more homogeneous the layer is. On the contrary, for higher gold thicknesses, when the layer is already electrically continuous, this difference is reversed.

b) Biopolymer nanostructures induced by argon plasma irradiation and metal sputtering

Physicochemical properties of polymer surface may be modified by many techniques based on various chemical or physical processes. Modification based on polymer surface exposure to plasma irradiation exhibits an easy and cheap technique for biopolymer surface nanostructuring. By plasma exposure of polymer surface combined with consequent heating or metal deposition can be prepared materials applicable both in tissue engineering as cell carriers, but also in integrated circuit manufacturing. The influence of argon plasma irradiation on PLLA (poly(L-lactide acid)) was presented. The combination of Ar⁺ particle irradiation, consequent sputter metallization and heating of biopolymer surface was summarized. Wettability of modified surface was characterized by the contact angle and surface energy determination. The surface morphology was studied using atomic force microscope and laser confocal microscope. The chemical analysis was performed using Rutherford Backscattering Spectroscopy (RBS) and X-ray Photoelectron Spectroscopy (XPS). The combination of plasma treatment with consequent thermal heating and/or metal sputtering led to the change of surface wettability, morphology and chemical structure. The surface roughness has been strongly influenced by the modification parameters, as well as the surface chemistry of biopolymer. The modification techniques had a positive effect on cell adhesion and proliferation.

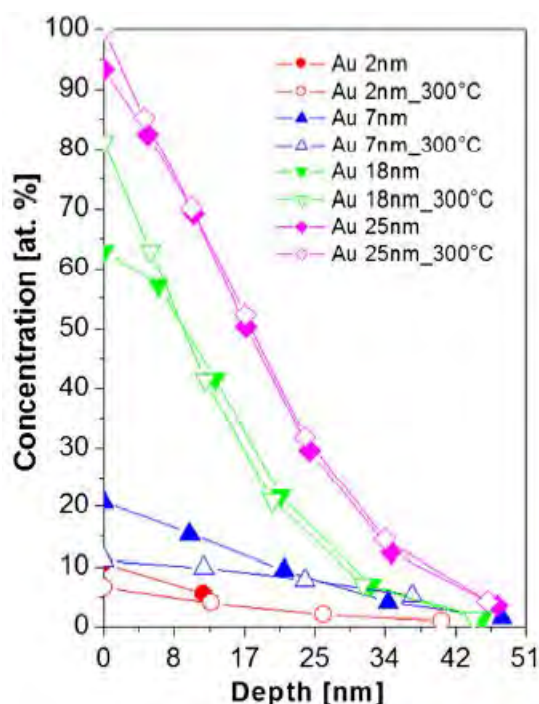


Figure 1 RBS spectra of gold structures evaporated on glass with room temperature and Au nanostructures evaporated on glass heated to 300°C (300°C).

PAPERS

1. A. Schaub, P. Slepíčka, I. Kašpárková, P. Malinský, A. Macková, V. Švorčík, *Gold nanolayer and nanocluster coatings induced by heat treatment and evaporation technique*, *Nanoscale Res. Lett.* 8 (2013) 249-257.

2. P. Slepíčka, P. Juřík, P. Malinský, A. Macková, N. Slepíčková Kasálková, V. Švorčík, *Biopolymer nanostructures induced by argon plasma irradiation and metal sputtering*, *NIM B*, 2013, under review.

CONFERENCES

1. P. Slepíčka, P. Juřík, P. Malinský, A. Macková, N. Slepíčková Kasálková, V. Švorčík, *Biopolymer nanostructures induced by argon plasma irradiation and metal sputtering*, IBA 2013 (Ion Beam Analysis), 23.6.-28.6. 2013, Seattle, USA.

2. N. Slepíčková Kasálková, P. Slepíčka, P. Malinský, A. Macková, V. Švorčík, *Surface changes of biopolymers induced by plasma treatment and acetone etching*, IBA 2013 (Ion Beam Analysis), 23.6.-28.6. 2013, Seattle, USA

Characterisation of minority phases in new Co-Re based alloys developed for gas turbine application

Neutron Physics Laboratory - Neutron diffraction

Ralph Gilles

Proposal ID

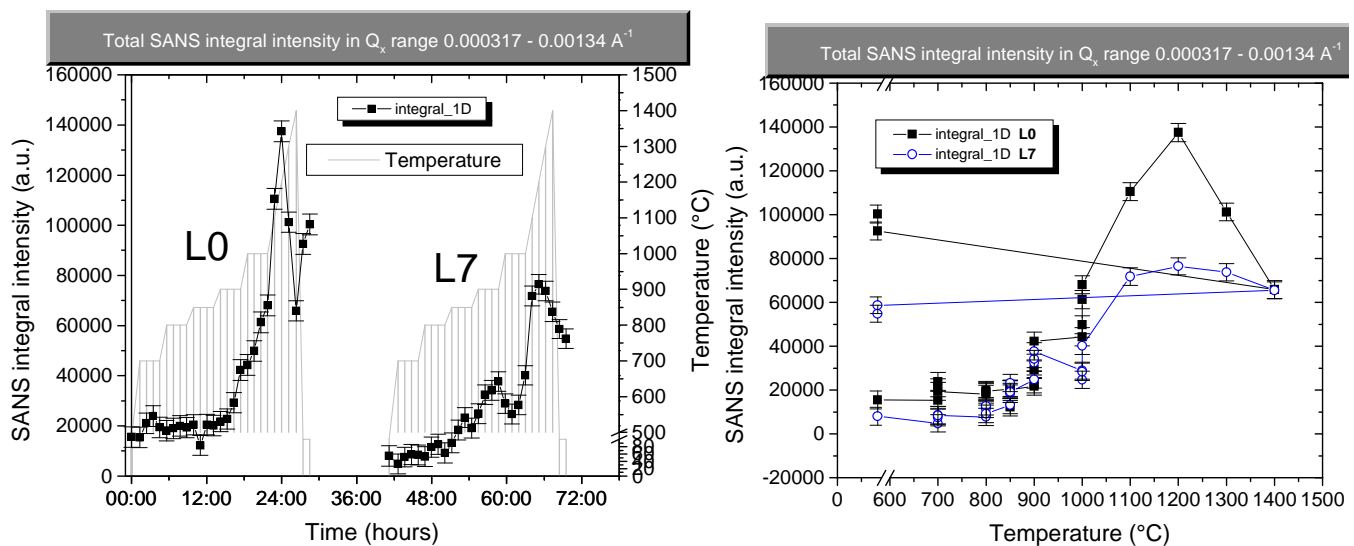
6

Characterisation of minority phases in new Co-Re based alloys developed for gas turbine application

The intended task of the experiment was to investigate sigma phase content and morphology changes in dependence on boron amount in the model ternary Co-17Re-23Cr alloy and to observe the evolution of sigma phase morphology with the temperature up to 1450°C. The characterization was carried out, the scattering from the sigma phase was, however, very low at RT due to the low scattering contrast. Therefore, there was only time to measure L7 and L0 at high temperatures (HT).

For the RT measurements of samples with various boron content, low (LR), medium (MR), high (HR) resolutions of the MAUD were subsequently used. Due to the very low scattering contrast, the scattering from the sigma phase was nearly negligible at RT. Therefore, no conclusions can be drawn from RT measurements on influence of boron content on sigma phase morphology at RT.

L0 (no boron) and L7 (200 ppm boron) samples measured at elevated temperatures. The temperature profiles for both samples were identical. Visible changes of intensity during temperature increase up to 1400°C were observed (see the figures).



For L0 (no boron), the increase of SANS intensity starts at 900°C (not before). It increases during the 4-hour hold at that temperature. Similarly, there is an increase at 1000°C. Further increase is visible at 1100°C and 1200°C (each 1 hour hold). Then, the intensity starts to decrease at 1300°C and 1400°C.

For L7 (boron), the increase of SANS intensity starts earlier, at 850°C. It increases during the 4-hour hold at that temperature. Similarly, there is a significant increase at 900°C. Then, there is “surprising” decrease at 1000°C followed by another increase at the end of 1000°C 4-hour hold and further at 1100°C and 1200°C (each 1 hour hold). Then, the intensity starts to decrease at 1300°C and 1400°C.

The results show that there exists an evolution of either sigma volume or morphology with temperature in both L0 and L7 samples. There also exists a difference in the evolution between L0 and L7 samples, which means that boron can have an influence on morphology.

Some of the scattering curves are being currently evaluated. It is necessary to look in detail onto evolution during the hold at 900°C and 1000°C to assess if some particle size evolution could be deduced. It, however, seems, that the increase of scattering comes from “larger” particles (over half micrometer in size).

Investigation of chemically modified carbon nanomaterials by Prompt-NAA

Neutron Physics Laboratory - Nuclear analytical methods with neutrons

Zdenek Sofer

Proposal ID

27

Project Title: **Investigation of chemically modified carbon nanomaterials by Prompt-NAA**

Proposer: Zdenek Sofer (zdenek.sofer@vscht.cz)

Lab: Neutron Physics Laboratory - Nuclear analytical methods with neutrons

The P-NAA method was used for characterization of various boron doped graphene materials. The boron doped graphene was synthesized by thermal exfoliation of various graphene oxide materials in the atmosphere of boron trifluoride diethyletherate. The incorporation of boron in graphene was investigated at various temperatures and carrier gas composition (N_2/H_2). Synthesized materials were characterized in order to evaluate chemical composition by elemental combustion analysis, X-ray photoelectron spectroscopy and X-ray fluorescence analysis. The boron content in the range of 20 – 560 ppm was measured by P-NAA method. The morphology of synthesized B-doped graphenes was investigated by scanning electron microscopy, transmission electron microscopy and atomic force microscopy. Transport properties were evaluated by four point probe resistivity measurement. According to rigid band model applied on these semiconductor materials we observed increase of resistivity due to the boron doping of graphene. The electrochemical performance of boron doped graphene was investigated using cyclic voltammetry in phosphate buffer (for inherent electrochemistry of B-doped graphene) and with various redox probes. The redox probes like $[Fe(CN)_6]^{3-/4-}$ was used to evaluate electron heterogeneous transfer rate on GC electrode modified with B-doped graphene. The capacitances of B-doped graphenes were evaluated from cyclic voltammetry in phosphate buffer solution. The weight specific capacitance of samples decreasing with increase of boron concentration.

The other graphene samples were prepared by chemical reduction of various graphene oxides with complex boron hydrides. The influence of graphene oxide composition on the concentration of remaining boron impurities in graphene was investigated. Significant differences were observed between graphene oxide prepared by Hofmann and Hummers methods. These results will be published in impacted journal within six months.

Published results:

1) L. Wang, Z. Sofer, P. Šimek, I. Tomandl, M. Pumera, Boron Doped Graphene: Scalable and Tunable p-Type Carrier Concentration Doping, The Journal of Physical Chemistry C, DOI: 10.1021/jp405169j.

2) H.L. Poh, P. Šimek, Z. Sofer, I. Tomandl, M. Pumera, Boron and nitrogen doping of graphene via thermal exfoliation of graphite oxide in a BF_3 or NH_3 atmosphere: contrasting properties, Journal of Materials Chemistry A, DOI: 10.1039/c3ta12460f.

Neutron diffraction on cobalt free Li-ion battery cathode materials

Neutron Physics Laboratory - Neutron diffraction

Veronika Zinth

Proposal ID

30

Neutron diffraction on cobalt free Li-ion battery cathode materials

Beamtime report

Veronika Zinth, Ralph Gilles, Premek Beran

New materials closely related to the well established NMC ($\text{LiNi}_{0.33}\text{Mn}_{0.33}\text{Co}_{0.33}\text{O}_2$) Li-ion battery material, with cobalt replaced by iron are currently studied and show promising capacities as well as cycling performance [1], [2]. To get a closer insight into structural details, $\text{Li}_{1+x}(\text{Ni}_{0.32}\text{Mn}_{0.32-y}\text{Fe}_{0.16})\text{O}_2$ samples with varying Li and Mn content were synthesized at FRM II, Germany and neutron diffraction pattern were collected at Meredith, UJF Nuclear Physics institute at a wavelength of 1.46 Å.

For $\text{Li}_{1.2}(\text{Ni}_{0.32}\text{Mn}_{0.32}\text{Fe}_{0.16})\text{O}_2$, Kartithkeyan et. al. [1] report a superstructure of the Li_2MnO_3 type in the space group $C2/m$ that arises from ordering of additional Li and Mn in the transition metal layers, indicated by superstructure reflections in the region $20\text{-}33^\circ 2\theta$ (Cu-radiation). However, the neutron pattern of our samples collected at Meredith gave no indication of such superstructure reflections. Therefore, Rietveld refinement of the data was performed in the $\alpha\text{-NaFeO}_2$ -type structure (space group $R\bar{3}m$, hexagonal setting). Figure 1 and Table 1 show the results of a joint Rietveld refinement of x-ray (top, Cu- $K\alpha_1$) and neutron data (bottom).

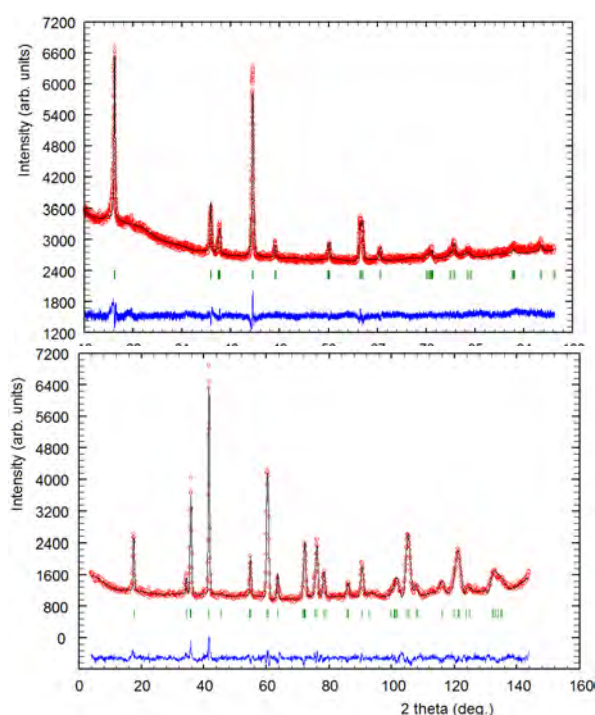


Figure 1:

Joint rietveld refinement of x-ray (Cu- $K\alpha_1$) (top) and neutron data (bottom) of $\text{Li}(\text{Ni}_{0.32}\text{Mn}_{0.28}\text{Fe}_{0.16})\text{O}_2$

Table 1: Structural information:

Space group: $R\bar{3}m$

Lattice parameters:

$a = 2.90188 \text{ \AA}$, $c = 14.34125 \text{ \AA}$

atom sites:

Li, Ni	3a	0 0 0
Ni, Mn, Fe, Li	3b	0 0 0.5
O	6c	0 0 0.24114

Since cation mixing (of Ni and Li) is known to influence the electrochemical properties of NMC type materials [3], special attention must be paid to the occupancies of the atomic sites. While the $3a$ site is mainly occupied by Li, some mixing of Ni and Li is expected because of the similar ionic radii of Ni^{2+} (0.69 Å) and Li^+ (0.76 Å) [1]. The refinement results suggest mixing of almost 13 % of Ni on the Li $3a$ site. On the $3b$ site, mixing of the transition metals Ni, Fe, Mn and of Li is found. With the assumption that the site is fully occupied, about 15 % Li occupy on this site. However, since no additional (superstructure) reflections can be observed in the diffraction pattern (Figure 1), the distribution of the transition metal ions and Li^+ seems to be statistical. Because four different elements occupy the $3b$ site, the Rietveld refinement alone can't give sufficient information to determine the occupancies of the transition metal ions and complementary information on the elemental composition (EDX, titration) that may help to develop a suitable model is currently collected.

To summarize, high quality neutron powder data was collected at Meredith $\text{Li}_{1+x}(\text{Ni}_{0.32}\text{Mn}_{0.32-y}\text{Fe}_{0.16})\text{O}_2$ lithium ion battery materials, giving an insight into structural details and the occupancies of the atomic sites that may help to understand the electrochemical properties.

1. Karthikeyan, K., et al., *Electrochimica Acta*, 2012. **68**: p. 246-253.
2. Lian, F., et al., *Journal of Applied Electrochemistry*, 2012. **42**(6): p. 409-417.
3. Zhang, X.Y., et al., *Journal of Power Sources*, 2010. **195**(5): p. 1292-1301.